

SYMMETRY-ADAPTED COMPUTATION: A CASE STUDY OF THE BUCHAREST DOME

Christopher M. Papadopoulos¹ and Marco T. LoRicco^{2,3}

ABSTRACT

Many important problems in civil engineering computation require the computation of solutions of nonlinear systems with symmetry, such as occurs in the large displacement post-buckling analysis of domes and reticulated structures. We describe the approach of symmetry-adapted computation, which provides not only (1) efficiency by reducing the number of degrees of freedom required to compute symmetric deformations with, but also (2) a systematic approach to computing buckling loads and corresponding buckled states (bifurcating solutions) that have reduced symmetry. In addition, we discuss further advantages of symmetry-adapted computation, such as (3) the ability to robustly compute zero eigenvalues of the tangent stiffness matrix, for detecting bifurcations (in many cases, this is unfeasible without symmetry-adapted computation); (4) the ability to simulate nearly-symmetric structures to identify critical imperfections, including those due to secondary and higher-order bifurcations; and (5) the ability to implement parallel processing. To demonstrate the method, as well as to provide a fresh analysis of a historically interesting case, we present initial results of our modeling and analysis of the “Bucharest Dome” (the National Economy Exhibition Pavilion in Bucharest), which was constructed in 1961 and collapsed in 1963.

KEY WORDS

symmetry-adapted computation, post-buckling analysis, elastic stability, imperfection analysis, symmetry-breaking bifurcation

INTRODUCTION

Symmetry principles are well established in mechanics and structural analysis. The common use of symmetry is restricted to assuming that the solutions of a symmetrical problem must also have the same symmetry. For example, consider a circular cylinder under the action of normal pressure on its lateral surface. A typical *linear* stress analysis of this cylinder assumes that the stress is a function only of distance r from the central axis. The tacit assumption is that deformations of the cylinder must inherit the initial circular

¹ Assistant Professor, Department of Civil Engineering and Mechanics, University of Wisconsin-Milwaukee, Milwaukee, WI, 53211, USA, Phone 414/229-3953, FAX 414/229-6958, cpapa@uwm.edu.

² PhD Candidate, Department of Civil Engineering and Mechanics, University of Wisconsin-Milwaukee, Milwaukee, WI, 53211, USA, Phone 414/229-2325, FAX 414/229-6958, mloricco@uwm.edu.

³ P.E., Project Engineer, Graef, Anhalt, Schloemer, and Associates, Inc., Milwaukee, WI, 53214, USA, Phone 414/266-9179, FAX 414/259-0037, Marco.LoRicco@GASAI.com.

symmetry. This reasoning is valid in linear analysis because solutions to (well-posed) linear problems exist and are unique, and since symmetric solutions exist, there can be no others.

In the context of *nonlinear* structural mechanics, however, multiple equilibrium states for a given loading condition typically exist. A *bifurcation point* is a point at which two distinct types of equilibrium states coincide (for example, at the transition from straight to bent). Nonlinear problems also admit equilibrium states that do not possess the complete symmetry of the governing conditions, although the entire *set* of solutions *does* possess the complete symmetry of the problem. The point at which an equilibrium state loses (*breaks*) symmetry often coincides with a loss of stability, as well as a bifurcation point⁴.

Large displacement and stability analysis of structural states inherently require nonlinear analysis⁵. This, in turn, requires numerical computation except in special cases since analytical solutions are unattainable or nonexistent. Nonlinear finite element analysis, in which deformations of continua are approximated by discrete displacements, is common.

A typical approach to computing solutions of nonlinear problems is called *path-following*, which we employ in our work. Path following makes use of the ansatz that solutions to nonlinear problems occur as one-dimensional curves in parameter-state space. For example, the equilibrium states of a column in compression consist of curves of the form $[\mathbf{u}, \lambda]$, where λ is the magnitude of the applied load (parameter), and \mathbf{u} is the vector of all displacements of specified points on the column (state). Path-following schemes have been developed and refined to provide numerically robust computation of solutions to a wide variety of nonlinear structural mechanics problems (Keller, 1977, 1982; Riks, 1984).

Solution paths of post-buckled states often arise as bifurcations from solution curves of pre-buckled states. This point of intersection, or bifurcation point, is necessarily a singular solution point of the governing equations (see, for example, Golubitsky and Schaeffer, 1984; Keller, 1977, 1982). Such singular points do not occur generically, but require special circumstances. Symmetry provides the conditions that give rise to bifurcations.

As a result, symmetry can be exploited in solving many structural mechanics problems in which multiple solutions are anticipated. A significant body of research has been dedicated to establishing the use of *symmetry-adapted computation* to solve nonlinear structural mechanics problems. An exhaustive review is beyond the scope of this paper, but we note several works whose approaches we follow (Healey, 1988; Healey and Treacy, 1991; Ikeda and Murota, 1991; Ikeda, Murota, and Fujii, 1991; Murota and Ikeda, 1991; Wohlever and Healey, 1995; Wohlever, 1996, 1999).

But why is symmetry-adapted computation useful, given that ‘real’ structures can never have perfect symmetry, even when symmetry is intended? Indeed, the crucial limiting

⁴ For example, consider the equilibrium solutions of a circular bar under axial compression. Assume that both the load and the bar possess perfect axial symmetry, and imperfections are absent. For compressive loads below the critical load, the equilibrium state of the rod is straight, and this state is stable. At greater loads, buckled solutions emerge and are now stable, while the straight solutions are unstable. A buckled solution clearly has *broken* the circular symmetry; however, the rotation of any buckled solution about the axis of the load is also a buckled solution, and thus the complete set of solutions has circular symmetry.

⁵ Although elementary approaches to studying structural stability, such as Euler buckling, make use of linear mechanical theories, even these approaches are tacitly nonlinear; they are based on using linearizing assumptions to large deformation states.

behaviors of structures occur as a result of *imperfections* that disturb the idealized symmetry, and even small imperfections can result in large reductions of structural load capacity. Symmetry-adapted computation is useful, therefore, to determine the solutions of the idealized symmetrical systems not as ends, but as guideposts against which to identify critical imperfections. Without symmetry-adapted computation, such critical imperfections would be difficult or impossible to systematically identify.

We attempt to demonstrate and advance the use of symmetry-adapted computation in structural analysis through the investigation of the collapse of the Bucharest Dome in 1963. This dome collapsed in a snowstorm while supporting only 30% of its design load. The investigators of the collapse have noted that a better understanding of the role of symmetry and asymmetric loading is required to understand the collapse (Soare, 1984; Beles and Soare, 1967). A further account of the Bucharest Dome is in Levy and Salvadori (1992). Our work will shed further light on this and similar matters.

COMPUTATIONAL PATH FOLLOWING

In general, the nonlinear finite element equations governing the static equilibrium of a structure can be expressed by the single vector equation

$$\mathbf{f}(\mathbf{u}, \lambda) = \mathbf{0}, \quad (1)$$

where $\mathbf{f}: \mathbf{R}^n \times \mathbf{R} \rightarrow \mathbf{R}^n$, \mathbf{u} is the n -dimensional vector of system displacements (where n is the number of degrees of freedom, or d.o.f.), and λ is the load parameter that measures the magnitude of an applied load vector. Solutions of (1) typically consist of one-dimensional curves of the form $[\mathbf{u}, \lambda] = [\mathbf{u}(s), \lambda(s)]$, where s is a measure of arc length along the curve. Schematic solutions, showing typical features, are depicted in Figure 1(a). Each solution point represents an equilibrium state of deformation corresponding to given load. Note that Figure 1(a) clearly illustrates the possibility that for a given load λ , more than one equilibrium state \mathbf{u} is possible.

The computation of solutions of (1) using a path-following scheme is based computing successive points $[\mathbf{u}, \lambda]_k = [\mathbf{u}(s_k), \lambda(s_k)]$ along a given solution path. An initial solution point is given, usually $[\mathbf{0}, 0]$, and further solutions are determined incrementally; the k th solution point is given by

$$[\mathbf{u}, \lambda]_k = [\mathbf{u}, \lambda]_{k-1} + [\Delta\mathbf{u}, \Delta\lambda]_{k-1}, \quad (2)$$

where the incremental quantities $\Delta\mathbf{u}_{k-1}$ and $\Delta\lambda_{k-1}$ are determined by the incremental form of Equation (1):

$$(\mathbf{K})_{k-1} (\Delta\mathbf{u})_{k-1} + (\mathbf{f}_\lambda)_{k-1} (\Delta\lambda)_{k-1} = \mathbf{0}, \quad (3)$$

where $\mathbf{K} = \mathbf{f}_\mathbf{u}$ is the system Jacobian, or tangent stiffness matrix.

A solution point $[\mathbf{u}, \lambda]$ at which \mathbf{K} is nonsingular is called a *regular point*. At regular points, (3) is solvable for $\Delta\mathbf{u}$ and $\Delta\lambda$, provided an auxiliary equation specifying the arc length condition

$$|\Delta\mathbf{u}|^2 + (\Delta\lambda)^2 = (\Delta s)^2, \quad (4)$$

although in practice, to avoid implicit equations, an approximation of (4) using previously computed solution points is used. At regular points, Newton's method can be applied to (3) in the determination of $[\Delta \mathbf{u}, \Delta \lambda]_{k-1}$, which takes the form

$$(\mathbf{K}_{k-1})^i (\Delta \mathbf{u})^i + (\mathbf{f}_{\lambda, k-1})^i (\Delta \lambda)^i = -(\mathbf{f}_{k-1})^i, \quad (5)$$

The iterates $[\mathbf{u}, \lambda]_k^i = [\mathbf{u}, \lambda]_{k-1}^i + [\Delta \mathbf{u}, \Delta \lambda]_{k-1}^i$ (k is fixed during each Newton iteration) are illustrated in Figure 1(b). Symmetry-adapted computation greatly improves the efficiency of solving the matrix computations required in (5).

A solution point $[\mathbf{u}, \lambda]$ at which \mathbf{K} is singular is called a *singular point*. Generically, a singular point at which \mathbf{f}_λ is in the range of \mathbf{K} is a bifurcation point, and a singular point at which \mathbf{f}_λ is not in the range of \mathbf{K} is a limit point. In Figure 1(a), bifurcation points are illustrated by points A and B , and a limit point is illustrated by point C .

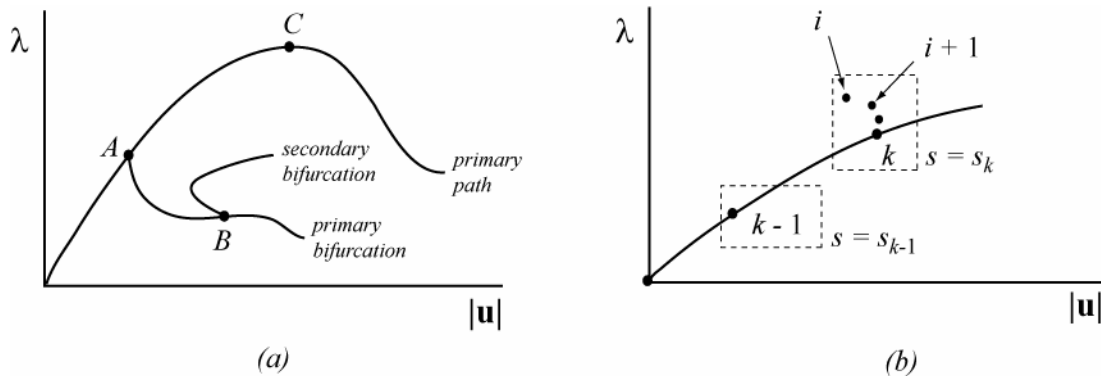


Figure 1. (a) Typical solutions of $\mathbf{f}(\mathbf{u}, \lambda) = \mathbf{0}$. (b) Schematic of Newton iteration procedure.

Generically, solution points are regular; singular points require special circumstances. Therefore, the path-following scheme outlined above is numerically well-conditioned at most points. Interestingly, however, even when a computed solution point is near a singular point, even though \mathbf{K} itself might be ill-conditioned, Keller (1977, 1982) demonstrated that path-following schemes are robust.

Bifurcation points typically lie between converged solution points. They are detected by tracking changes in the number of negative eigenvalues of \mathbf{K} between converged solution points; when such changes are detected, the precise location of the bifurcation point is determined by interpolation. While in principle this is straightforward, many numerical difficulties arise in practice when several bifurcation points exist between two given computed solution points. One of the great benefits of symmetry-adapted computation is the ability to compute such eigenvalues accurately, efficiently, and robustly. General computational schemes will likely not converge to any eigenvalues in such circumstances.

SYMMETRY-ADAPTED COMPUTATION

Mathematically, symmetries are characterized by *groups*. If the system governed by (1) has symmetry corresponding to a group G , then each element g of G can be represented by an

orthogonal $n \times n$ matrix Γ_g ; the set of these matrices forms a *representation* of the group G over \mathbf{R}^n . The function \mathbf{f} in the governing equation (1) is then *equivariant* with respect to G , and which means that \mathbf{f} satisfies the following relationship:

$$\mathbf{f}(\Gamma_g \mathbf{u}, \lambda) = \Gamma_g \mathbf{f}(\mathbf{u}, \lambda) \tag{6}$$

for all g in G . Notice that if a displacement vector \mathbf{u} is symmetric with respect to the group G , then $\mathbf{u} = \Gamma_g \mathbf{u}$, for all g in G , and (6) implies that $\mathbf{f}(\Gamma_g \mathbf{u}, \lambda) = \Gamma_g \mathbf{f}(\mathbf{u}, \lambda) = \mathbf{f}(\mathbf{u}, \lambda)$, i.e. \mathbf{f} maps symmetric states to symmetric states. As a consequence, solution points on a path containing $[\mathbf{0}, 0]$ all have complete G -symmetry, since $\mathbf{0}$ is G -symmetric. These results agree with common experience in which structural responses possess the full symmetry of the given problem, and because the symmetric solutions are a (small) subspace of all solutions, they require fewer computations.

Results from group representation theory provide for the decomposition of \mathbf{R}^n into p mutually orthogonal subspaces:

$$\mathbf{R}^n = \sum_{\mu=1}^p \oplus \mathbf{V}^\mu \tag{7}$$

We note that \mathbf{V}^1 ($\mu = 1$) is the space of G -symmetric states. The number p and the dimension n_μ of \mathbf{V}^μ depend on both the dimension n and fundamental properties of the group (p is the number of irreducible characters of the group G); clearly, $\sum_{\mu=1}^p n_\mu = n$, and for each subspace \mathbf{V}^μ , there exists a matrix \mathbf{Q}^μ , of dimension $n \times n_\mu$, whose columns are orthogonal basis vectors for \mathbf{V}^μ . It follows that the assembled orthogonal matrix $\mathbf{Q} = [\mathbf{Q}^1 \mathbf{Q}^2 \dots \mathbf{Q}^p]$ is a change of basis matrix on \mathbf{R}^n . Further background on the theoretical underpinnings is given in Hammermesh (1989); Healey (1988); and Ikeda, Murota, and Fujii (1991).

An important class of symmetry that is relevant to structural problems is dihedral symmetry. The dihedral group $D-N$ characterizes the symmetries of a regular N -gon. The Bucharest Dome has dihedral symmetry $D-128$. Algorithms to construct the matrices \mathbf{Q}^μ are provided in Ikeda and Murota (1991) and Murota and Ikeda (1991).

As an example, consider an equilateral triangle in the plane, constructed of three rigid links connected by hinges, which clearly has 6 d.o.f. Any displacement \mathbf{u} can be expanded in terms of a standard Cartesian basis at each node: $\mathbf{u} = x_1 \mathbf{e}_1 + x_2 \mathbf{e}_2 + \dots + x_6 \mathbf{e}_6$. In the symmetry-adapted basis, $\mathbf{u} = u_1 \mathbf{b}_1 + u_2 \mathbf{b}_2 + \dots + u_6 \mathbf{b}_6$. These bases are depicted in Figure 2, below, and explicitly given in equation (*).

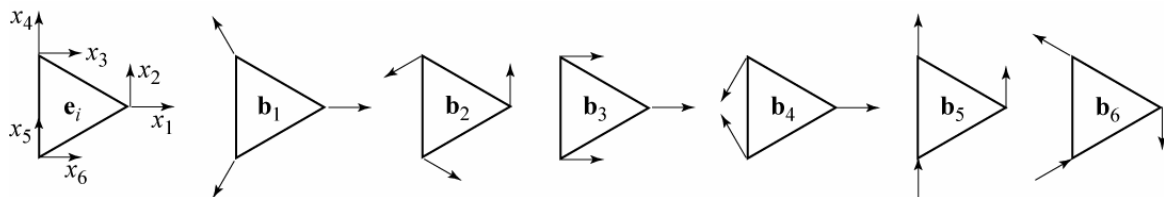


Figure 2. Left figure: Standard Cartesian Basis, with all 6 d.o.f. sketched simultaneously.
 Right 6 figures: Symmetry-adapted Basis, with each d.o.f. sketched separately.

$$[\mathbf{e}_1 \mathbf{e}_2 \mathbf{e}_3 \mathbf{e}_4 \mathbf{e}_5 \mathbf{e}_6] = \begin{bmatrix} 1 & & & & & \\ & 1 & & & & \\ & & 1 & & & \\ & & & 1 & & \\ & & & & 1 & \\ & & & & & 1 \end{bmatrix}, \quad [\mathbf{b}_1 \mathbf{b}_2 \mathbf{b}_3 \mathbf{b}_4 \mathbf{b}_5 \mathbf{b}_6] = \begin{bmatrix} \frac{\sqrt{3}}{3} & & \frac{\sqrt{3}}{3} & \frac{\sqrt{3}}{3} & & \\ & \frac{\sqrt{3}}{3} & & & \frac{\sqrt{3}}{3} & -\frac{\sqrt{3}}{3} \\ -\frac{\sqrt{3}}{6} & -\frac{1}{2} & \frac{\sqrt{3}}{3} & -\frac{\sqrt{3}}{6} & & -\frac{1}{3} \\ \frac{1}{6} & -\frac{\sqrt{3}}{2} & & -\frac{1}{6} & \frac{\sqrt{3}}{3} & \frac{2}{3} \\ \frac{2}{6} & \frac{1}{6} & \frac{\sqrt{3}}{3} & -\frac{\sqrt{3}}{6} & & \frac{1}{6} \\ -\frac{\sqrt{3}}{6} & \frac{1}{2} & \frac{\sqrt{3}}{3} & -\frac{\sqrt{3}}{6} & & \frac{1}{3} \\ \frac{1}{6} & -\frac{\sqrt{3}}{2} & & -\frac{1}{6} & \frac{\sqrt{3}}{3} & \frac{2}{3} \\ -\frac{\sqrt{3}}{6} & \frac{1}{2} & \frac{\sqrt{3}}{3} & -\frac{\sqrt{3}}{6} & & \frac{1}{6} \\ \frac{2}{6} & \frac{1}{6} & \frac{\sqrt{3}}{3} & -\frac{\sqrt{3}}{6} & & \frac{1}{6} \\ -\frac{\sqrt{3}}{6} & -\frac{1}{2} & \frac{\sqrt{3}}{3} & -\frac{\sqrt{3}}{6} & & -\frac{1}{3} \\ \frac{1}{6} & \frac{\sqrt{3}}{2} & & \frac{1}{6} & \frac{\sqrt{3}}{3} & \frac{2}{3} \\ \frac{2}{6} & \frac{1}{6} & \frac{\sqrt{3}}{3} & -\frac{\sqrt{3}}{6} & & \frac{1}{6} \end{bmatrix} \quad (*)$$

The symmetry transformation matrices for this example are as follows: $\mathbf{Q}^1 = [\mathbf{b}_1]$, $\mathbf{Q}^2 = [\mathbf{b}_2]$, $\mathbf{Q}^3 = [\mathbf{b}_3 \mathbf{b}_4]$, and $\mathbf{Q}^4 = [\mathbf{b}_5 \mathbf{b}_6]$.

A striking and powerful result of group representation theory is that when evaluated at a symmetric state \mathbf{u} , the Jacobian can be transformed such that it becomes decoupled (block diagonalized) in direct correspondence with the symmetry subspaces; that is,

$$\mathbf{Q}^T \mathbf{K} \mathbf{Q} = \tilde{\mathbf{K}} = \begin{bmatrix} \tilde{\mathbf{K}}^1 & & & \\ & \tilde{\mathbf{K}}^2 & & \\ & & \ddots & \\ & & & \tilde{\mathbf{K}}^p \end{bmatrix}, \quad \text{where } \tilde{\mathbf{K}}^\mu = (\mathbf{Q}^\mu)^T \mathbf{K} \mathbf{Q}^\mu \quad (8)$$

Note that the resulting *stiffness block matrices* $\tilde{\mathbf{K}}^\mu$ are of dimension $n_\mu \times n_\mu$, and because \mathbf{Q}^1 projects onto the fully symmetric subspace, the computation of $\Delta \mathbf{u}$ in (5) requires only data with the full symmetry; therefore, the matrix equations required to solve (5), $\mathbf{K}\{\mathbf{x}, \mathbf{y}\} = \{-\mathbf{f}, -\mathbf{f}_\lambda\}$ are now decoupled, and can be solved more efficiently:

$$(\mathbf{Q}^1)^T \mathbf{K} (\mathbf{Q}^1) \mathbf{Q}^1 \{\mathbf{x}, \mathbf{y}\} = (\mathbf{Q}^1)^T \{-\mathbf{f}, -\mathbf{f}_\lambda\} \Leftrightarrow \tilde{\mathbf{K}}^1 \{\tilde{\mathbf{x}}, \tilde{\mathbf{y}}\} = \{-\tilde{\mathbf{f}}, -\tilde{\mathbf{f}}_\lambda\} \quad (9)$$

An example of (8, 9) corresponding to the equilateral triangle is illustrated in Figure 3.

A further – and perhaps more important – advantage of the decoupling (8) is the vastly improved ability to determine bifurcation points. When two distinct bifurcation points are close together, two distinct eigenvalues are then nearly zero. In problems with many d.o.f., determining (and distinguishing) these eigenvalues using the entire stiffness matrix \mathbf{K} will lead to convergence problems. In the decoupled case, these distinct eigenvalues belong to distinct blocks, eliminating convergence problems. Moreover, because the blocks are much smaller in size than the entire stiffness matrix, the computational effort is much less. Finally, the process of determining eigenvalues using the symmetry blocks can be done in parallel, because the distinct blocks can be analyzed independently.

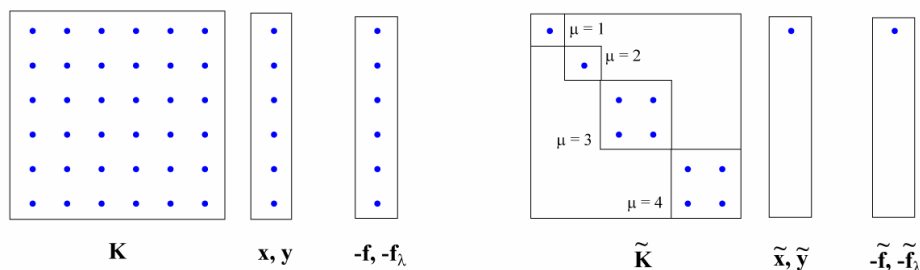


Figure 3. Matrix Calculations in Standard (left) and Symmetry-adapted (right) Bases.

MODELING AND ANALYSIS OF THE BUCHAREST DOME

When completed in 1961, the Bucharest Dome, designed by Dr. Ferdinand Lederer, was a daringly light structure that was technically acclaimed. The dome's structure consisted of a lattice of hollow steel tubes (102 mm diameter, 6 mm thick) that outlined a spherical surface of radius 65 m. The dome rose to 19 m at its center, and spanned a base diameter of 93 m. The dome's lattice had a 17 m diameter circular hole at the top, the circumference of which consisted of a stiff compression ring (steel box girder) and supported a 25 ton lantern. The total dead weight of the structure, cladding, lantern, and fixtures was approximately 430 tons. These and other construction and design details can be found in Soare (1963).

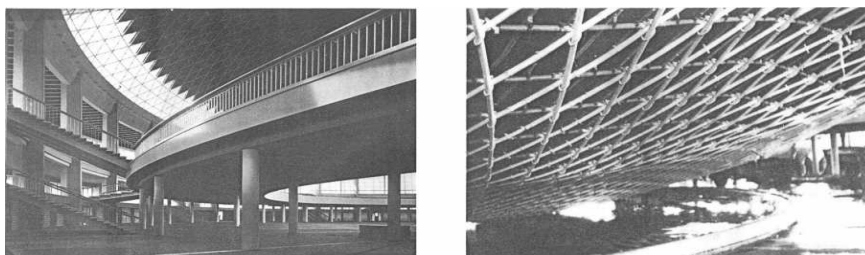


Figure 4. Photos of Bucharest Dome from inside, before (left) and after (right) collapse.

The Bucharest Dome collapsed only 17 months after its completion, under a non-uniform snow load of approximately 200 tons, concentrated along 5 radial lines. Figure 4 provides photographs of the dome before and after collapse. Strikingly, 200 tons represented only 30% of the design load for uneven snow load. Even though the designers considered elastic stability, the investigators of the collapse believed that this premature load failure was due to asymmetrical loading, and recommended further work to understand this phenomenon better (Soare, 1984; Beles and Soare, 1967). We seek to explore this matter further.

Computational tools necessary to simulate the behavior of the lattice were not available to the designers. As the dominating mechanism in the members of the Bucharest Dome is axial force, and the corresponding dominant mechanism is a shell is membrane stress, an 'equivalent' shell model was substituted for the lattice by smearing the entire structural material uniformly over the spherical surface of the dome, with corrections to account for bending at the edges of the dome. Based on this analogy, the equivalent shell thickness for

the Bucharest Dome is about $t = 0.003$ m, which is prohibitively thin (the spherical radius of the dome is $R = 65.25$ m, whence $t/R < 1/20,000$!).

Nevertheless, the lattice is not a shell, and because its members also have bending stiffness, it can perform essentially as designed. We believe that further subtleties regarding stability are responsible for the dome's collapse.

The specialized symmetry-adapted algorithms necessary for our study are provided by a computer code ContCM, originally written by Wohlever (1999). ContCM provides for two basic element types, a truss element, and a "Simo" shell element for 'moderately thin' shells. Given the extremely thin nature of the equivalent shell, we modeled the dome as a lattice with the same geometry as the original dome ($D-128$ symmetry, 37 circumferential rings, 4736 nodes, 14208 d.o.f., 13824 truss elements), as illustrated in Figure 5.

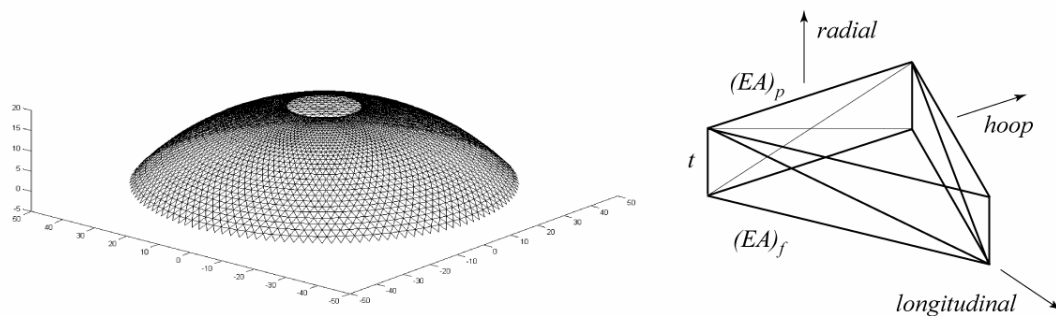


Figure 5. Model of Bucharest Dome (left) and Detail of Double-layer Truss (right).

However, because the truss elements in ContCM are axial elements only, we modeled the Bucharest Dome as an equivalent double-layer truss, consisting of a main framework ("f") and a pseudo framework ("p"). A sketch of this double-layer model is provided in Figure 5. We calibrated this model to have the equivalent axial stiffness and moment of inertia (about the mid-plane) as the original steel tubes. The resulting separation between the layers, t , was determined to be $t = 0.040$ m. The double-layer model has 28416 d.o.f. and 50688 elements.

After building the model in ContCM, we performed a load-displacement analysis on the dome using its self-weight (including the lantern weight) as the input load vector; snow loads have not yet been considered. The load factor λ measures the proportion of this load applied at a given solution point (e.g. $\lambda = 1$ represents the total self-weight, $\lambda = 2$ represents twice self-weight, etc.) Our calculations to date include the following: (1) computation of the primary solution path ($D-128$ symmetric), (2) determination of bifurcation points along the primary path, and (3) the computation of a bifurcation path ($D-64$ symmetric). Note that item (1) is possible, but much less efficient, using standard Cartesian coordinates, for the entire stiffness matrix \mathbf{K} is of size 28416×28416 , whereas the stiffness block associated with the computation of the $D-128$ solution path is 296×296 . [We estimate the symmetry calculations in this case to be 100 time faster than those in Cartesian coordinates. Detailed discussion of computing efficiency is in Wohlever, 1999; and Ikeda and Murota, 1991]. Items (2) and (3) are intractable using Cartesian coordinates, and require the use of symmetry-adapted computation.

CONCLUSIONS AND FUTURE WORK

Figure 7 summarizes the numerical results. The primary solution path represents equilibrium states that maintain the full $D-128$ symmetry of the structure; solutions along this path exhibit essentially linear behavior until reaching the limit load at approximately $\lambda = 3.09$ (1330 tons). The first bifurcation point occurs at $\lambda = 1.09$, after which point the primary solutions become unstable. This finding is questionable, for the dome should not become unstable at slightly above its self-weight. Further calibration, such as by comparing our results with those of commercial finite element software will help to correct some of the results that appear questionable. Still, given that the dome suffered an unexpected collapse, in the range of $\lambda \sim 1.5$, our initial results seem to reveal clues about its weaknesses.

As we continue to study this problem, we will systematically compute solutions corresponding to the other bifurcation points on the primary path, and we will study the effect of imperfections to determine further limitations on load capacity. For example, based on the computed path for $D-64$ symmetry, small geometrical imperfections with $D-64$ symmetry would likely reduce the limit load to roughly $\lambda = 2$. We will also investigate the importance of secondary bifurcations, the importance of which is described by Healey (1989). We will also consider the effect of several unbalanced snow loads to simulate the effect that caused the dome's collapse. Finally, we will consider developing a new rod element for ContCM that has both axial and bending stiffness; such an element will provide a useful comparison to, and possibly a more realistic model than, our double-layer model.

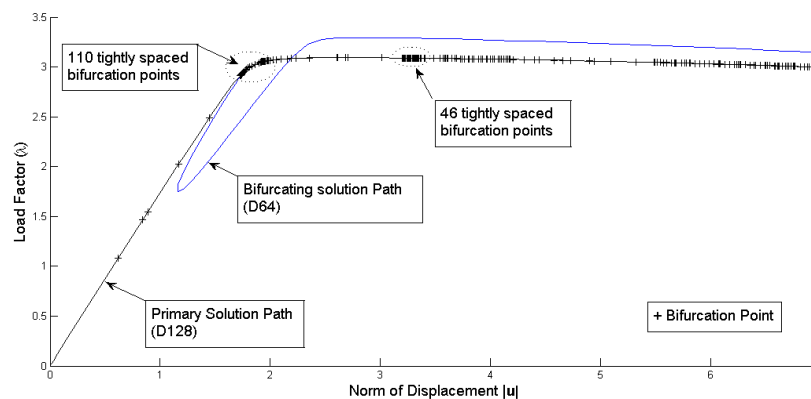


Figure 7. Computed Solutions and Bifurcation Points for Bucharest Dome.

ACKNOWLEDGMENTS

The authors express their appreciation to the Graduate School at the University of Wisconsin-Milwaukee for providing support for this work.

REFERENCES

- Beles, A.A., and Soare, M.V. (1967). "Some Observations on the Failure of a Dome of Great Span." In R.M. Davies (editor), *Space Structures, Proc. 1st Int. Conf. Space Struct., University of Surrey, 1966*, 419-423.

- Golubitsky, M., and Schaeffer, D.G. (1984). *Singularities and Groups in Bifurcation Theory*, Vol. I. Springer-Verlag, New York.
- Hamermesh, M. (1989). *Group Theory and its Application to Physical Problems*. Dover, New York.
- Healey, T.J. (1988). "A Group Theoretic Approach to Computational Bifurcation Problems with Symmetry." *Comp. Meth. Appl. Mech. Engin.*, 67 257-295, 1988.
- Healey, T.J. (1989). "Why Bifurcation: A study of a Reticulated Dome." In A.H.-S. Ang (editor), *Structural Design, Analysis, and Testing*, 942-948. American Society of Civil Engineers, New York.
- Healey, T.J. and Treacy, J.A. (1991). "Exact Block Diagonalization of Large Eigenvalue Problems for Structures with Symmetry." *Int. J. Numer. Meths. Engin.*, 31 265-285.
- Ikeda, K. and Murota, K. (1991). "Bifurcation Analysis of Symmetric Structures using Block Diagonalization." *Comp. Meth. Appl. Mech. Engin.*, 86 215-243.
- Ikeda, K., Murota, K., and Fujii, H. (1991). "Bifurcation Hierarchy of Symmetric Structures." *Int. J. Sol. Struct.*, 27 (12) 1551-1573.
- Keller, H.B. (1977). "Numerical Solution of Bifurcation and Nonlinear Eigenvalue Problems." In Paul. H. Rabinowitz (editor), *Applications of Bifurcation Theory*, 359-384. Academic Press, New York.
- Keller, H.B. (1982). "Practical Procedures in Path Following Near Limit Points." In R. Glowinski and J.L. Lions (editors), *Computing Methods in Applied Sciences and Engineering*, Vol. V, 177-183. North-Holland, Amsterdam.
- Levy, M. and Salvadori, M. (1992). *Why Buildings Fall Down*. Norton, New York.
- Murota, K., and Ikeda, K. (1991). "Computational use of Group Theory in Bifurcation Hierarchy Analysis of Symmetric Structures." SIAM, *J. Scientific and Statistical Computing*, 12 (2) 273-297.
- Riks, E. (1984). "Some Computational Aspects of the Stability Analysis of Nonlinear Structures." *Comp. Meth. Appl. Mech. Engin.*, 47 219-259.
- Soare, M.V. (1984). "Investigation of the Collapse of a Large-span Braced Dome." In Z.S. Makowski (editor), *Analysis, Design and Construction of Braced Domes*, Ch. 5. Nichols Publishing Company, New York.
- Soare, M. (1963). "The Metallic Lattice Dome of the National Economy Exhibition Pavilion at Bucharest." In N. Esquillan and Y. Saillard (editors), *Hanging Roofs, Proc. IASS Colloquium on Hanging Roofs, Continous Metallic Shell Roofs, and Superficial Lattice Roofs, Paris, 1962*, 276-287. North-Holland, Amsterdam.
- Wohlever, J.C. and Healey, T.J. (1995). "A Group Theoretic Approach to the Global Bifurcation Analysis of an Axially-compressed Cylindrical Shell." *Comp. Meth. Appl. Mech. Engin.*, 122 315-349.
- Wohlever, J.C. (1997). *User Manual for ContCM and MMContCM: Release 1.0*. Unpublished manuscript, Cornell University.
- Wohlever, J.C. (1999). "Some Computational Aspects of a Group Theoretic Finite Element Approach to the Buckling and Postbuckling Analyses of Plates and Shells of Revolution." *Comp. Meth. Appl. Mech. Engin.*, 170 373-406.